Natural killer cell-derived exosome-entrapped paclitaxel can enhance its anti-tumor effect

D. HAN¹, K. WANG¹, T. ZHANG², G.-C. GAO¹, H. XU¹

Abstract. – OBJECTIVE: To study the effectiveness of natural killer cell-derived exosome (NK-Exos)-entrapped paclitaxel (PTX-NK-Exos) in enhancing its anti-tumor effect.

MATERIALS AND METHODS: The NK-Exos were isolated through ultra-high-speed centrifugation, and the PTX-NK-Exos system was constructed via electroporation. The morphology, particle size, Zeta potential and entrapment rate of PTX-NK-Exos were evaluated using transmission electron microscope (TEM), dynamic light scattering (DLS), Western blotting and high-performance liquid chromatography (HPLC) spectively. The uptake of Exos in human cancer MCF-7 cells was observed und ser confocal microscope. Moreover, the ct of PTX-NK-Exos on MCF-7 cell viability determined through methyl thiazolyl tetra um (MTT) assay, flow cytometra amidino-2-phenylindole (DAP) The e fects of PTX-NK-Exos on m **Jeng** onucle of B-cell ic acid (mRNA) and protein pressio ociate lymphoma-2 (Bcl-2), Bcl otein (Bax) and Caspase-3 MC ed using quantitatiy verse ription-polyn (qRT-PC Western merase chain rea blotting, respeg

os were s cessful-**RESULTS:** eed centrifugation, ly isolated via ultra-h and they uniform pa size and high expression markers for Exc F-7 cells could exos. The PTX-NK-Exos drug delivery take was s essfully prepared using elecsys TX group and NK-Exos group, trop n of MQ cells declined, the nuthe pr dent and the apoptosis was r apo se compared with those in TX group and PTX-NK-Exos the migration of MCF-7 cells declined that in Control group. Accordults of gRT-PCR and Western blotg, PTX-NK-Exos exerted an anti-tumor effect gh inducing the up-regulation of Bax and e-3 in the apoptotic signaling pathway in cells.

CONCLUSIONS: Exos isolated through ultrahigh-speed centrifugation can be used to prepare the PTX -Exos on allive system through electronic pration. Drug Exos can effectively represent the confidence of th

Ko

xosomes, MCF-7 cells, Apoptosis.

troduction

Breast cancer is a major disease in females be world, with such biological characas strong invasiveness, and proneness to recurrence and metastasis. Currently, chemotherapy is still one of the most common therapeutic methods for various tumors. Paclitaxel (PTX), an important chemotherapy drug for tumor, is a kind of basic drug for the clinical treatment of advanced and early ovarian cancer, breast cancer, lung cancer, etc.¹, but its wide clinical application is limited due to its poor water solubility. Although the mixture of castor oil and ethanol (1:1) can dissolve paclitaxel, the dose-dependent toxicity caused by such solvent cannot be ignored. In particular, the biological and pharmacological properties of castor oil can lead to allergic reaction, hyperlipidemia, abnormal lipoprotein pattern, erythrocyte aggregation, and long-term irreversible neurogenic disease².

To solve the above problems, Abraxane[®], a castor oil-free albumin-bound PTX nano preparation, was approved for marketing by the US Food and Drug Administration in 2005, which displays good pharmacokinetics³ and therapeutic effects⁴. In phase III clinical trial for women with metastatic breast cancer, Abraxane[®] has a better therapeutic effect than castor oil-based PTX, but there are still significant declines in leukocytes and erythrocytes and allergic reaction when it is

¹Jiaxing University, Jiaxing, Zhejiang, China

²Zhejiang Chinese Medical University, Hangzhou, Zhejiang, China

administered via intravenous injection⁵. Therefore, the new drug-loading system is essential for expanding the clinical application of PTX.

Currently, the most commonly used drug carriers are mostly synthesized artificially, such as polymeric drug carriers, causing problems with biocompatibility. Exosomes (Exos) are derived from cells or organisms themselves, and their biocompatibility is undoubtedly excellent compared with other artificially synthesized carriers. Moreover, the related proteins on the surface of Exos are beneficial to the cell phagocytosis, so Exos, as drug carriers, have aroused increasingly more attention and research. Sun et al⁶ entrapped the hydrophobic drug curcumin using Exos to improve its solubility and bioavailability, and transnasally delivered the drug to the brain for the treatment of cerebral inflammation. Alvarez-Erviti et al⁷ entrapped small-interfering ribonucleic acid (siRNA) into Exos via electroporation and delivered siRNA to the brain after surface targeted modification. In addition, Agrawal et al⁸ proved that the milk-derived Exos can entrap PTX and compared with free PTX (30%) at the same dose, the Exos-entrapped system has tumor inhibition rate of 60% and mild to effects.

Most importantly, Exos will specifically the RNA, protein and other components in pa cells during secretion, and reach recific si through body fluid transport ed in th in vivo signal transduction e escape or imi berefore, ases^{9,10} and treatment of related the source and physiologic determine that the tents c by Exos are different, and the v related unctions are to the parent co terature reported in that natural ved Exos (NK-Exos) er ce can inhibit he abnormal feration of melanoma cells d raise the survi te of melanoma mice sed on this, with NK-Los as the carrier of I entrapped into NK-Exos using eleci In this experiment. It was found -entrap that N PTX (PTX-NK-Exos) ficanti the proliferation of breast a better therapeutic effect. cells a

terials and Methods

ents

MCF-7 cells were purchased from Shanghai Cell Bank, Chinese Academy of Sciences, fetal bovine serum (FBS), minimum essential medium-α (MEMα), high-glucose Dulbecco's Modified Eagle's Medium (DMEM) and double antibodies from Gibco (Rockville, MD, USA), TJ Invitrogen (Carlsbad, CA, USA), 63, An and TSG101 antibodies from m, mRNA extraction kit and SYBR Greek kit from Shanghai BAT Biotechnology Co Shanghai, China), chloroform ycerol, nol isopropanol and glacial tic acid (anal pure) from Sinophar hemical Reagent Ltd. (Beijing, China ai 🛭 Spirit Biotwin pe (TE) transmission elegation from Thermo Fisher entific (USA), Beckman L ultra-high frigerated centrifuge by Beckma. Miami, FL, sizer Nano ZS90. USA), and Malver

Cellure

S was taken and centrifuged at 120,000 g for and 5% present tate at the bottom of tube was deed to obt Exos-free FBS. After sterilization in the control of the control of

NK-92 cells were cultured in the MEMα con-10% Exos-free FBS, and MCF-7 cells are dured in the DMEM containing 10% FBS and 1% double antibodies. They were all routinely cultured in the constant temperature and humidity sterile incubator with 5% CO₂ at 37°C, and the medium was replaced regularly, followed by subculture when 85-90% cells were fused.

Extraction of Exos

Exos were extracted through ultra-high-speed differential centrifugation 14,15: The culture supernatant was collected and centrifuged at 300 g for 10 min, 2,000 g for 10 min and 10,000 g for 30 min to remove cells and cell debris. After filtering through the 0.22 µm filter membrane, the filtrate was centrifuged at 120,000 g for 2 h, and the supernatant was discarded. Then, the precipitate was resuspended with an appropriate amount of Exos-free phosphate-buffered saline (PBS), and centrifuged at 120,000 g for another 2 h to remove the residual protein. After the concentration of Exos was measured with bicinchoninic acid (BCA) method (Beyotime, Shanghai, China), Exos were stored at -80°C for later use.

Drug Entrapment

A total of 0.2 μL of Exos and 50 μg of PTX (Taxol) were mixed evenly with buffer (200 μL

system), electroporated at room temperature under 1000 V for 20 ms and stored at 4°C¹6. Then, the blank-NK-Exos (Control group) and PTX-NK-Exos (Experimental group) were obtained.

Identification of Exos

Observation of morphology of Exos under the TEM: $20~\mu L$ of Exos obtained using ultra-high-speed centrifugation, PEG precipitation and kit were taken, added dropwise onto the copper mesh, and sucked dry using the filter paper after 1 min. Then, a drop of 1% uranyl acetate was added and sucked dry using the filter paper after 1 min. After drying under the incandescent lamp, Exos were observed and photographed under the TEM.

Determination of Exos particle size via dynamic light scattering (DLS): 0.5 mL of Exos mother liquor was taken, added with 4.5 mL of ultrapure water, and filtered with the 0.22 μ m filter membrane. Finally, the particle size was detected using the Malvern Zetasizer Nano ZS90.

Analysis of Exos specific proteins using Western blotting: the separated and purified Exos were added with 5× loading buffer, boiled at 100°C for 5 min and cooled to room temperature. After aration via 12% sodium dodecyl sulpha the acrylamide gel electrophoresis (SDS-PAO protein in the gel was transferred onto the vinylidene difluoride (PVDF) membranes (N h 5% sk pore, Billerica, MA, USA), seale milk powder at room temper h, an incubated with rabbit antian TS monoit antihan Alix clonal antibody (1:1000) monoclonal antibody 4:10 (000) at 4°C man CD63 monocle antibe overnight. After hed with nembrane w Tris-Buffered 3ST) (5 th Tween-2 was incubated again $\min \times 3$ time the p HRP)-labeled goat with hors dish peroxic anti-rab gG secondary a. y at room temperati or 2 h, and the memorane was washed ith TP $(5 \text{ min} \times 3 \text{ times})$. Finally, the aga ected using the super enhanced prote chemilu cence (Pierce, Rockford, IL, kit.

An esis of Exes Uptake Under the Language of the State of the Control of the Cont

labeled with the PKH67 Green orescent Cell Linker Kit dye. NK-Exos were ended in 1 mL of diluent C, and PKH67 dye a final concentration of 4×10⁶ mol/L was freshly prepared. According to the instructions, 1 mL of NK-Exos was added into 1 mL of dye

for incubation in the dark at room temperature for 4 min, and the staining was terminated using 2 mL of bovine serum albumin (BSA) (0.5%). The labeled NK-Exos were centrifu at 120,000 g for 2 h to remove the aual dy The precipitate was resuspended 1 200 μL of PBS. The above dye-labeled NK were added into a 24-well plate with slides riginal concentration of 20 μg/m incuba r 12 \sim (5 min \times h. After washing with with 10% PFA to NK-Exos were incub min in the dark, and xati was aspirated. ► PB 1×3 tip , 500 After washing w lindo! μL of 4',6-di dino-2-(DAPI) ch well for aining for was added in 10 min, ap PI dye was rated. After $\sin \times 3$ times), 100 μ L of washing with PB F-actin (cytoskeletor ning) was added into for incubation 10 min in the dark, then F-actin was aspirated. After washing h PBS (5 m \times 3 times), the slides were ed with ant orescence quenching buffer. lides prepared were acquired nages of a al microscope and analyzed una using I oftware.

ion of Effect of PTX on on ation of MCF-7 Cells Using MTT Assay

 4×10^4 MCF-7 cells were inoculated into a 96-well plate. After adherence to the wall, the cells were added with blank NK-Exos (40 μg/mL), Taxol solution (The dose of PTX was 15 μg/mL), PTX-NK-Exos (PTX concentration: 15 μg/mL) and blank control (Control) without any treatment, respectively, with 6 replicates in each group. The culture plate was incubated in the incubator with 5% CO₂ at 37°C for 24, 48, and 72 h, and then, 20 μL of MTT solution was added into each well and placed in the incubator for 4 h. After the supernatant was discarded, 150 μL of DMSO solution was added into each well, and the optical density (OD) value was measured at 490 nm using a microplate reader.

Detection of Apoptosis of MCF-7 Cells Via DAPI Staining

 5×10^5 MCF-7 cells were inoculated into a 6-well plate. After adherence to the wall, the cells were added with blank NK-Exos (40 $\mu g/mL$), Taxol solution (The dose of PTX was 15 $\mu g/mL$), PTX-NK-Exos (PTX concentration: 15 $\mu g/mL$) and blank control (Control) without any treatment, respectively, with 3 replicates in each group.

Determination of Apoptosis Rate Through Annexin V-FITC/PI Double Staining

5×10⁵ MCF-7 cells were inoculated into the 6-well plate. After adherence to the wall, the cells were added with blank NK-Exos (40 µg/ mL), Taxol solution (The dose of PTX was 15 ug/mL), PTX-NK-Exos (PTX concentration: 15 μg/mL) and blank control (Control) without any treatment, respectively, with 3 replicates in each group. After culture for 24 h, the cells were digested with EDTA-free trypsin, centrifuged at 1,000 rpm for 8 min, resuspended with 400 µL of Annexin V binding buffer, and transferred into the 1.5 mL EP tube (Eppendorf, Hamburg, Germany). Then 5 µL of Annexin-FITC staining solution was added and mixed evenly for incubation for 15 min in the dark. Finally, 10 µL of propidium iodide (PI) staining solution was added for incubation for 5 min in the dark, followed by detection using the flow cytometer.

Detection of Cell Migration Ability Via Wound Healing Assay

The culture plate without inoculated cells was marked. After digestion, the cells were in ed into the 24-well plate, and added wit NK-Exos (40 µg/mL), Taxol solution (Th se of PTX was 15 µg/mL), PTX-NK-Exos concentration: 15 µg/mL) and blank control (trol) without any treatment, res h of treatment, while PBS w Contro group, with 3 replicates in fter the n grou cells fully covered the be of plat bev were scratched using a 1 pl p lar to the plate (try me width of ensure each scratch). The ution was he cell cult aspirated, and was washe th PBS cell debris and photofor 3 times to ash of graphed (I After cult. another 24 h, the cell mig on was observe photographed again 4). Finally, the cell stratch length was d usir mageJ software, and the cell me as calculated: cell migration rate migi th - T2 (%) = (dth/T0 width × 100%. peated for 3 times. xperi

Cells in each group were lysed with TRIzol lysis buffer, and the total RNA was extracted and

synthesized into cDNA according to the instructions. Then, qRT-PCR was performed under the following reaction system: 5 µL of SYBR Tag enzyme, 1 µL of forward primers and verse primers of Bax, Bcl-2 and Cas e-3, 1 μ of cDNA template, and RNase-fr water added until the constant volume of 25 µ total of 40 cycles. The qRT-PCR results were a d using 2-ΔΔCt method. Primer seque own s used below: Bax-F: GGCTGGAC 5'-CA GACT-3'; Bax-R: 5' AGTAC GAGAGO GCCGT-3'. Bcl-2-F: TTC TTCGGTGG-CAAA GGTCA-3'; Bcl-2 • 5 BAGpase-3-1 GGC GCCGCA-3'. TCTG-TA-3'; Casp 5'-GCT-**GTTTTCGT GCATCG** TACC-3'. GAPDH-F: AAGCTCA-3'; ACTT 5'-CGAC GAP-DH-R: 5'-ACTGAG GCAGGGACTC-3'.

Bax, Bcl-2, and Caspase-3 in MCF-7 "Is Through Yestern Blotting

s were w ed with PBS and lysed with unop pitation assay (RIPA; Beyotime, 51 China) lysis buffer to extract the fal protein in each group. 30 μg of proteins in were loaded, subjected to 12% SDSransferred onto the membrane, sealed with 5% skim milk powder solution for 1 h and incubated with Bax, Bcl-2 and Caspase-3 primary antibodies at 4°C overnight. On the next day, the membrane was washed with TBST (5 min \times 3 times), and ECL reagent (mixture of solution A and solution B at 1:1) was added for exposure. Finally, the gray value of each band was analyzed using ImageJ software.

Statistical Analysis

All experiments were repeated for at least 3 times, and SPSS 17.0 (SPSS Inc., Chicago, IL, USA) software was used for data processing. Measurement data were expressed as mean ± standard deviation. Comparison between multiple groups was done using One-way ANOVA test followed by post-hoc test (Least Significant Difference). *p*<0.05 suggested that the difference was statistically significant.

Results

Identification of Exos

Results of TEM revealed that the particle size of Exos obtained via ultra-high-speed centrif-

ugation was about 100 nm (Figure 1A, 1B), consistent with that (30-150 nm) reported in the literature. It could be observed via staining that Exos had intact capsule structure in a typical cup shape. In addition, drug-loaded Exos had no significant changes in the morphology (Figure 1B), and they had evident saucer-like double-layer membrane structure, with single distribution or aggregation in groups, and the background was clear with less pollutants.

The particle sizes of NK-Exos and PTX-NK-Exos were detected via DLS (Nano ZS90). As shown in Figure 1C, both mean and median particle sizes of NK-Exos were about 100 they ranged from 80 to 110, confirm s that th particle size of Exos was within definition. After drug loading, the particle PTX-NK-Exos was slightly increased (Figure consistent with the results in the drug rature. loading, the particle size NK-Exos rose

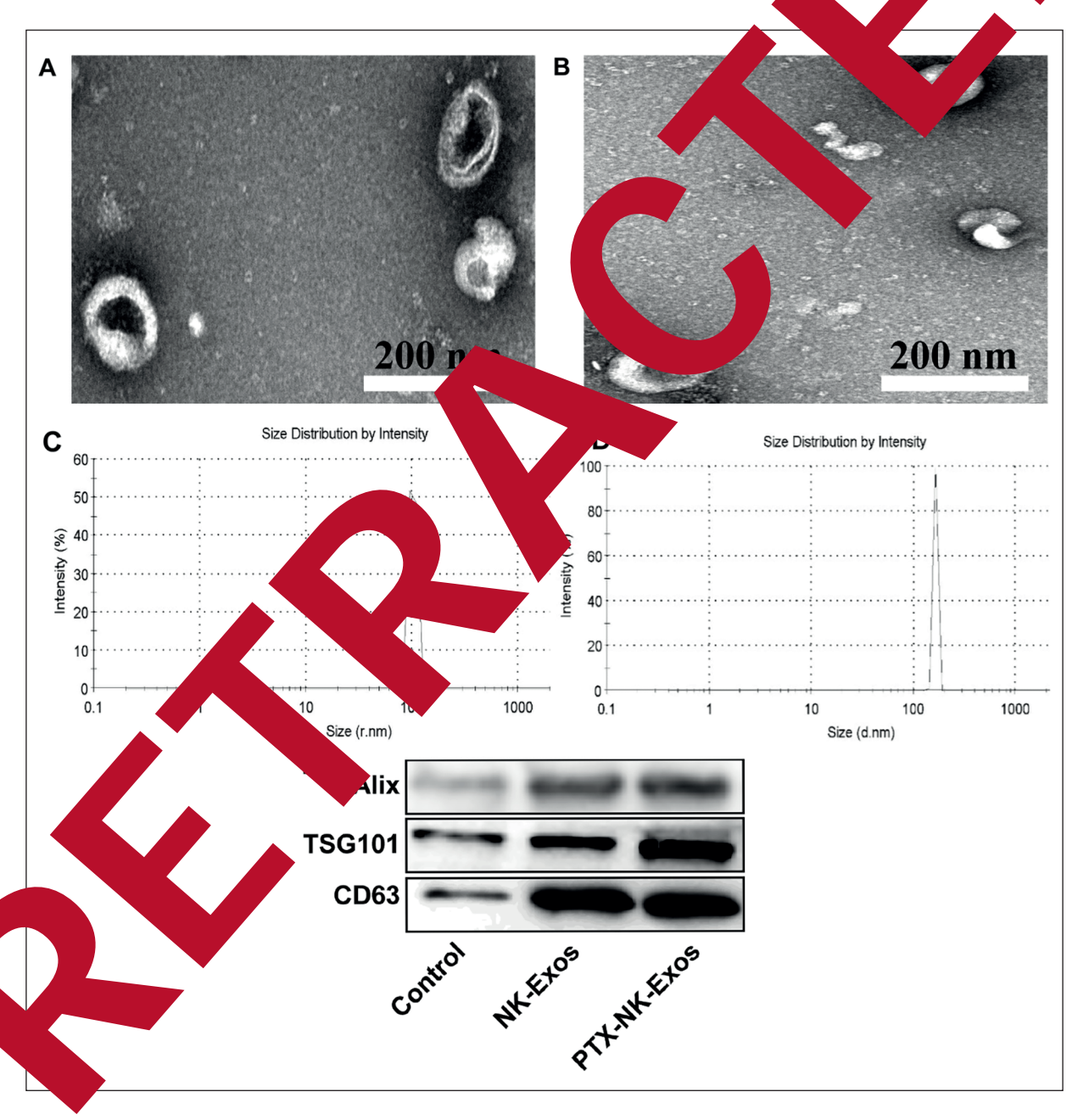


Figure 1. Identification of Exos. **A, B,** Morphology of Exos observed by TEM (magnification: 20, 000 ×). **C, D,** Particle size of NK-Exos analyzed using DLS. **E,** Expressions of Exos specific proteins analyzed using Western blotting.

because of the embedding of PTX into lipid bilayer of Exos and surface adsorption caused by hydrophobic effect^{8,17}.

The expressions of Exos specific marker proteins were determined using Western blotting, including membrane protein CD63 and inclusion proteins Alix and TSG101 (Figure 1E). It was found that CD6, Alix and TSG101 had positive and significantly higher expressions, suggesting that Exos were obtained via ultra-high-speed centrifugation. There was no evident effect on the expressions of Exos specific proteins after drug loading.

Uptake of Exos

As shown in Figure 2, the blue DAPI indicated the nucleus, the red phalloidine indicated the cytoskeleton, and the green PKH67 indicated the Exos. In the Merge graph, green fluorescence was clearly visible, mainly in the cytoplasm. The 4T1 cytoskeletal protein F-actin stained by phalloidine was labeled with Rhodamine 123, and red fluorescence could also be clearly seen in 4T1, indicating that PKH-67-labeled Exos can be taken in by MCF-7 cells.

PTX-NK-Exos Promoted Apoptosis MCF-7 Cells

According to the results of MTT assay ure 3A-3C), the MCF-7 cell viability signific ly declined in PTX group and $\frac{1}{2}$ Exos grocompared with that in Contact at 24 h 48 h and 72 h (*p<0.05, *p<0.05, *p<0.05). The MCF-7 cell viability also a ficantly clined in

PTX-NK-Exos group compared with that in PTX group. (##p<0.01, ##p<0.01, ##p<0.01). Moreover, the results of DAPI staining and flow cytometry (Figure 3D-3F), consistent with those assay, showed that the inhibitory ef s of PT and PTX-NK-Exos at the same c entration on proliferation of MCF-7 cells w re significant than that of free PTX /*p < 0. t there was no significant difference in the tory effect on proliferation 1CF-7 cells NK-Exos and PTX.

Effect of PTX-NY-Ex- ligration Ability of MY Cells

The result around healing an anifested that the many control of MCF- alls declined in NK-Ex s group of PTX group compared with that in Control on (*p<0.05), while it was a tily decreased TX-NK-Exos group copared with that in FTX group (*p<0.01) gure 4).

Expressions Bax, Bcl-2, and Caspa. MCF-7 Cells

According to the results of qRT-PCR (Figure the mRNA expressions of Bax, Bcl-2 pase-3 in MCF-7 cells remarkably rose in NK-Exos group and PTX group compared with those in Control group (*p<0.05), while they were also remarkably up-regulated in PTX-NK-Exos group compared with those in PTX group (*p<0.01).

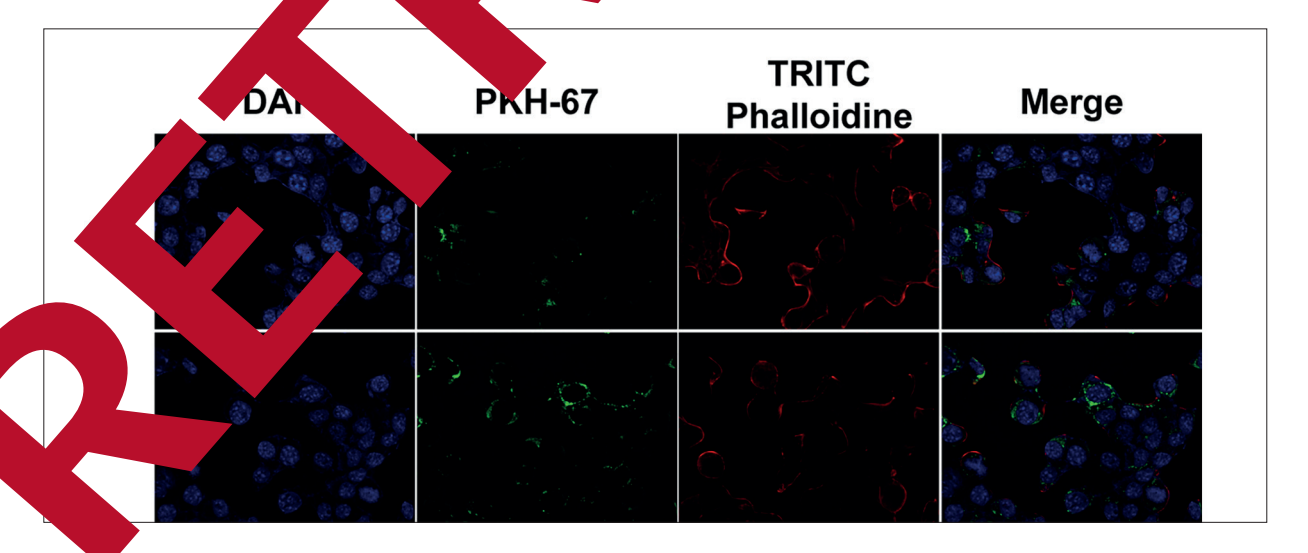


Figure 2. Uptake of Exos. Uptake of Exos in MCF-7 cells is observed using the laser confocal microscope. DAPI-stained nuclei, PKH67-stained Exos, and Rhodamine-labeled phalloidine-stained cytoskeleton (magnification: 400 ×).

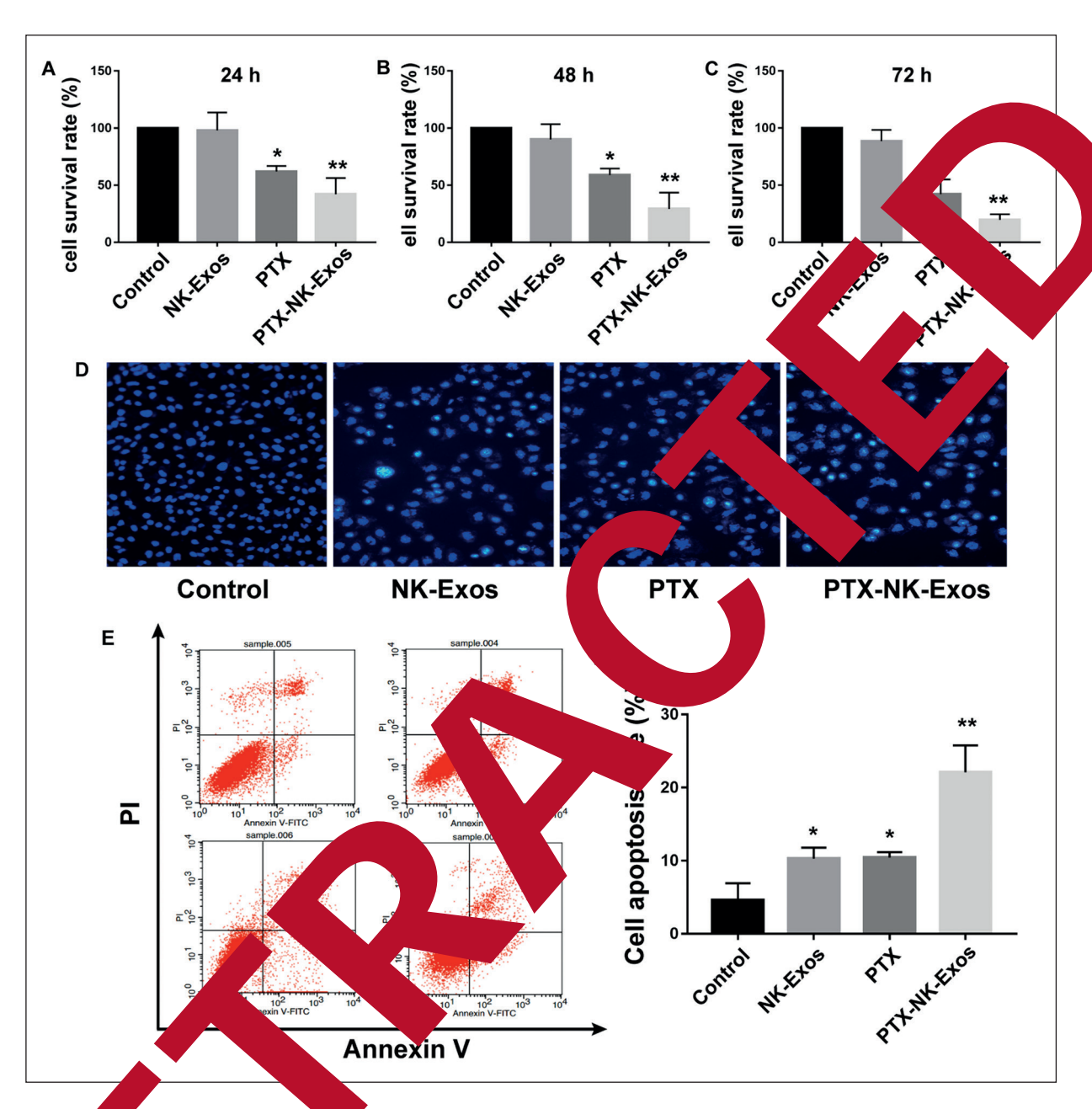


Figure MCF-7 cell apoptosis assa, A-C, Survival rate of MCF-7 cells at 24 h, 48 h and 72 h detected using MTT assay. D, Apoptosis of MCF cells detected using DAPI staining (magnification: 100 ×). E, F, Apoptosis rate of MCF-7 cells after drug admitted to the detected using flow cytometry.

ts o. N exos on Protein L. ssions ax, Bcl-2, and Can se-3 in ACF-7 Cells

Caspase-3 in MCF-7 cells remarkably rose in control group (*p<0.05), while they were also remarkably up-regulated in PTX-NK-Exos group compared with those in PTX group (*p<0.01).

Discussion

PTX is a kind of important anti-tumor drug that plays an important role in the treatment of various malignant tumors, such as breast cancer⁸. However, the dose-dependent toxicity of PTX greatly restricts its widespread application in clinic. In recent years, the naturally sourced nanoscale drug carrier Exos has been used to deliver a variety of chemotherapy drugs to spe-

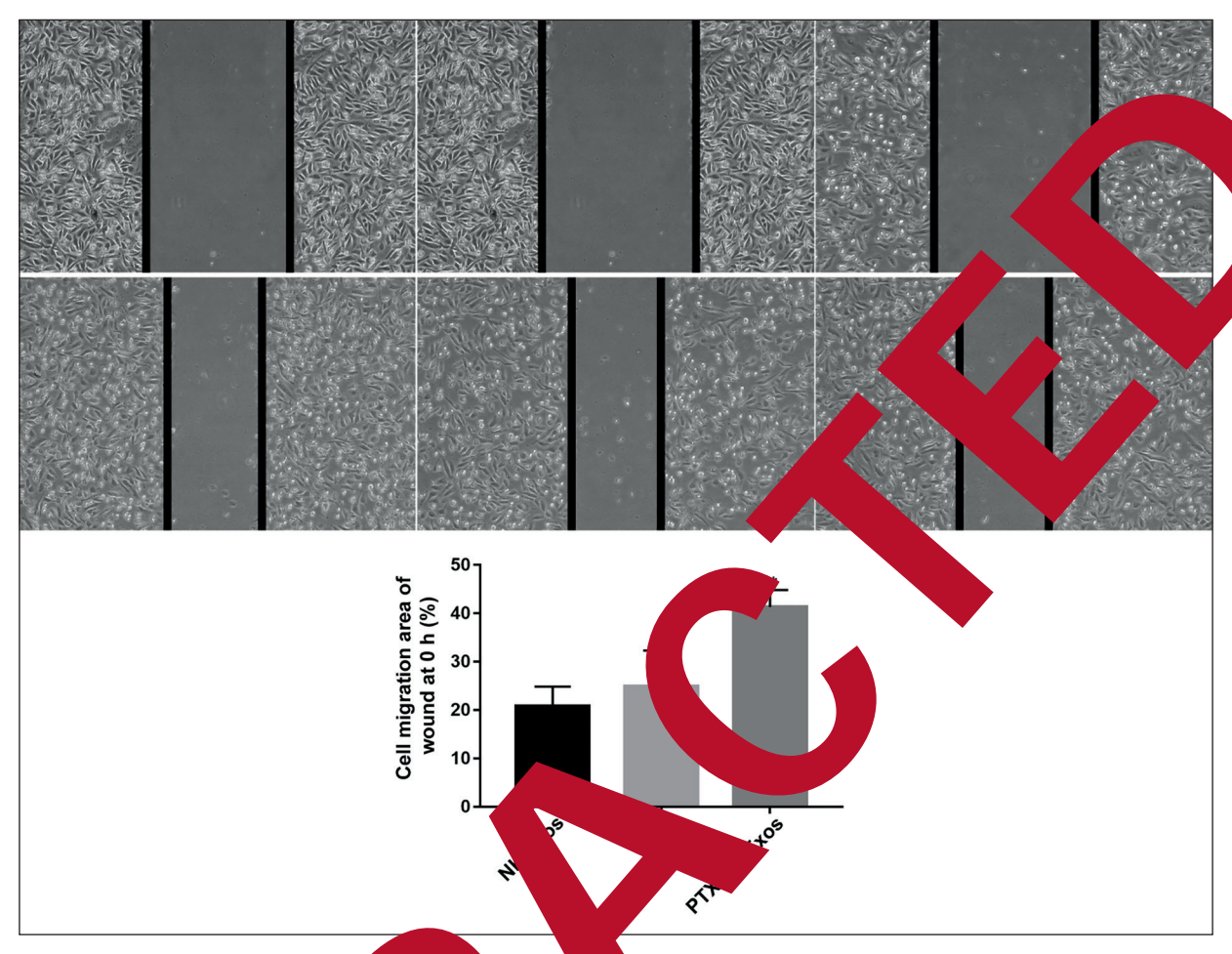


Figure 4. PTX-NK-Exos inhibits (CF-7 cell and gnification: 50 ×).

cific tissues and cells in vi tissues¹⁹. Exos pos the pl es of parent cells, and its role otercellular unication and signal tra has attrac ncreas-Van et al¹⁷ found that ingly more a ation umor tissue. Exos from regulate the tumor sponse, facilitat immung tumor metastanduce the resistance of tumor cells to sis, a ugs. Exos isolated from milk che herapy anti-tup or activity^{22,23}, and NKhas side ef cs on melanoma cells in Exos ha found in the research for Mor os can significantly inhibit growth in vivo²⁴. At the same time, Exos tun matibility and it is widely explored arrier, which can simultaneously very hydrophobic and hydrophilic cargos. s, NK-Exos itself can exert an inhibitory on melanoma. Therefore, NK-Exos were used as the delivery system for PTX in this study.

In this investigation, the PTX-NK-Exos delivery system was successfully prepared. The particle size of Exos was first detected via DLS before and after drug loading. It was found that the mean particle size of Exos was increased from 104 nm to 141.6 nm after drug loading. Yuan et al¹⁸ have shown that PTX will be partially embedded in the lipid bilayer of Exos during entrapment, resulting in a slight increase in the particle size of Exos after drug loading. To determine the effect of drug loading on the property of Exos, the surface protein, morphology and potential of Exos were further evaluated. The results of Western blotting manifested that the drug loading process did not affect the protein abundance of Exos. The TEM results showed that after drug loading, the morphology and structure of Exos basically remained unchanged, but its potential slightly declined, consistent with the results obtained by other researchers^{18,25}. Therefore, the drug loading process has

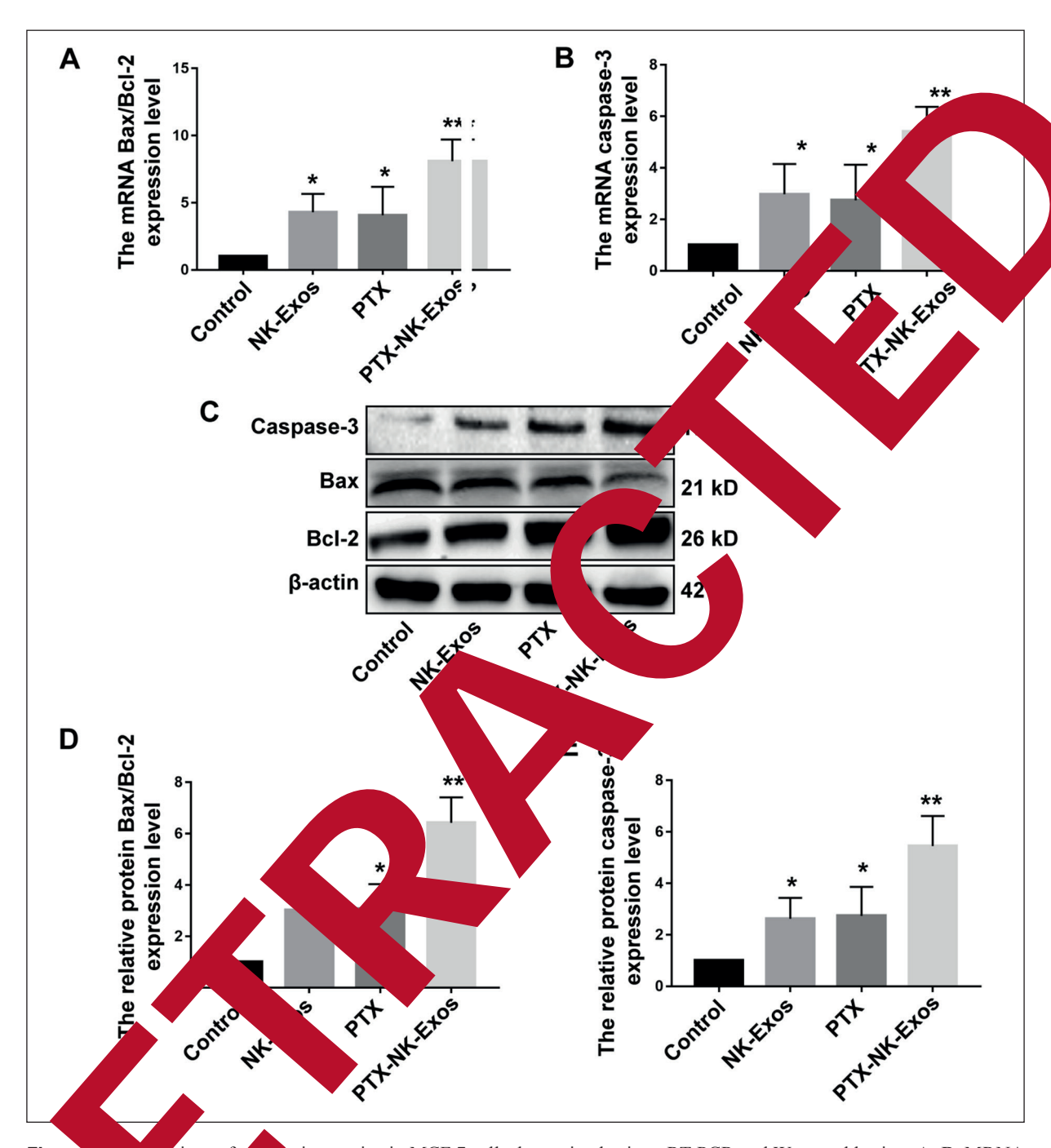


Figure sions of colors proteins in MCF-7 cells determined using qRT-PCR and Western blotting. A, B, MRNA and Colors are 3 in MCF-7 cells detected via qRT-PCR. C-E, Protein levels of Bax, Bcl-2 and Caspase-3 in Cells are vestern blotting.

ecture of Exos, and all properties of Exos are yed after drug loading.

PTX-NK-Exos drug loading system at the same dose had a higher inhibition rate on human breast

cancer MCF-7 cells compared with free PTX. Such a phenomenon has been explained by some studies, and it has been found that the lipid bilayer of Exos can directly target and fuse cells, thereby enhancing cellular internalization of PTX and improving the therapeutic effect. However, there

are some limitations. This procedure cannot be used for all drugs. Electroporation is traditionally considered as means to introduce DNA, RNA, enzymes, drugs or biochemical reagents into cells. Generally, RNAs and other hydrophilic compounds can be loaded into exosomes by electroporation. The principle of this method is to create countless pores on the exosome membrane under short and high-voltage pulses, thus allowing the penetration of drug molecules into the exosomes. Taxol is a kind of important anti-tumor drug that plays an important role in the treatment of breast cancer. However, the dose-dependent toxicity of PTX greatly restricts its widespread application in clinic. NK-exosomes exhibited toxic effects on melanoma cells in vitro. Moreover, it has reported that NK-exosomes can significantly inhibit the tumor growth in vivo. So, when Taxol was carried by NK-exosomes, low-dose taxol has better antitumor effect^{7,24-27}.

Conclusions

In this paper, with the clinically widely PTX as a model drug, NK-Exos were ed from NK cells via classical ultra-high centrifugation and used as the PTX de system. The PTX-NK-Exos system was prep via electroporation, so that the ry syste of chemotherapy drugs carri al carr ver, the er was constructed succe ıly. Ma ug deli carrier was extracted, the system was prepared, and the vitro pharmacodyn activ evaluated, thereby further v activity ging the and of drug loading

Confl¹ of Interest

The ors declarathat they have no conflict of interests.

ding will ements

nental A search Project of Zhejiang Science and hnology De ment

References

 VANG P, WANG H, HUANG Q, PENG C, YAO L, CHEN H, QIU Z, WU Y, WANG L, CHEN W. Exosomes from M1-Polarized macrophages enhance paclitaxel

- antitumor activity by activating macrophages-mediated inflammation. Theranostics 2019; 9: 1714-1727
- GELDERBLOM H, VERWEIJ J, NOOTER K, SPAN Cremophor EL: the drawbacks and a mage vehicle selection for drug formulation Eur J Cancer 2001; 37: 1590-1598.
- SPARREBOOM A, SCRIPTURE CD, TRIES AMS PJ, DE T, YANG A, BEALS B, FIGG W Desai N. Comparative preclinical clinica acokinetics of a cremoph ee, nanopart (BI-007) min-bound paclitax and par hor (Ta formulated in Cra Clin Can Res 2005; 11: 4136
- GRADISHAR W. son N H, De-ANDIN SAI N, BHAG J. Phase 1AWKINS M, paclitaxel III trial of particle albu oil-based pacompa lvethylated ca h breast cancer. J Clin Oncol ı won clitax 2005; 23: 7794-7
- WE, CHIDLOW BHARALI DJ, Mousa SA. atticals. Nanomedicine 2008; 4: 273-282.
- Sun D, Zhua C, Xiang X, Liu Y, Zhang S, Liu C, Barnes S, Grid W, Miller D, Zhang HG. A novdrug delivery system: the anactivity of curcumin is enhanced with collaboration and activity of curcumin is enhanced with collaboration. In the collaboration of the collab
- MJ. Delivery of siRNA to the mouse brain by systemic injection of targeted exosomes. Nat Biotechnol 2011; 29: 341-345.
- AGRAWAL AK, AOIL F, JEYABALAN J, SPENCER WA, BECK J, GACHUKI BW, ALHAKEEM SS, OBEN K, MUNAGALA R, BONDADA S, GUPTA RC. Milk-derived exosomes for oral delivery of paclitaxel. Nanomedicine-Uk 2017; 13: 1627-1636.
- 9) Peinado H, Aleckovic M, Lavotshkin S, Matei I, Costa-Silva B, Moreno-Bueno G, Hergueta-Redondo M, Williams C, Garcia-Santos G, Ghajar C, Nitadori-Hoshino A, Hoffman C, Badal K, Garcia BA, Callahan MK, Yuan J, Martins VR, Skog J, Kaplan RN, Brady MS, Wolchok JD, Chapman PB, Kang Y, Bromberg J, Lyden D. Melanoma exosomes educate bone marrow progenitor cells toward a pro-metastatic phenotype through MET. Nat Med 2012; 18: 883-891.
- 10) Andreola G, Rivoltini L, Castelli C, Huber V, Perego P, Deho P, Souarcina P, Accornero P, Lozupone F, Lugini L, Stringaro A, Molinari A, Arancia G, Gentile M, Parmiani G, Fais S. Induction of lymphocyte apoptosis by tumor cell secretion of Fasl-bearing microvesicles. J Exp Med 2002; 195: 1303-1316.
- 11) EITAN E, ZHANG S, WITWER KW, MATTSON MP. Extracellular vesicle-depleted fetal bovine and human sera have reduced capacity to support cell growth. J Extracell Vesicles 2015; 4: 26373.
- Yu G, Jung H, Kang YY, Mok H. Comparative evaluation of cell- and serum-derived exosomes to

- deliver immune stimulators to lymph nodes. Biomaterials 2018; 162: 71-81.
- ZHANG Y, LIU Y, LIU H, TANG WH. Exosomes: biogenesis, biologic function and clinical potential. Cell Biosci 2019; 9: 19.
- 14) LUNAVAT TR, JANG SC, NILSSON L, PARK HT, REPISKA G, LASSER C, NILSSON JA, GHO YS, LOTVALL J. RNAi delivery by exosome-mimetic nanovesicles - implications for targeting c-Myc in cancer. Biomaterials 2016; 102: 231-238.
- 15) Du W, Zhang K, Zhang S, Wang R, Nie Y, Tao H, Han Z, Liang L, Wang D, Liu J, Liu N, Han Z, Kong D, Zhao Q, Li Z. Enhanced proangiogenic potential of mesenchymal stem cell-derived exosomes stimulated by a nitric oxide releasing polymer. Biomaterials 2017; 133: 70-81.
- 16) WLASCHEK M, TANTCHEVA-POOR I, NADERI L, MA W, SCHNEIDER LA, RAZI-WOLF Z, SCHULLER J, SCHARFFET-TER-KOCHANEK K. Solar UV irradiation and dermal photoaging. J Photochem Photobiol B 2001; 63: 41-51.
- 17) WAN Y, WANG L, ZHU C, ZHENG Q, WANG G, TONG J, FANG Y, XIA Y, CHENG G, HE X, ZHENG SY. Aptamer-conjugated extracellular nanovesicles for targeted drug delivery. Cancer Res 2018; 78: 798-808
- 18) Yuan D, Zhao Y, Banks WA, Bullock KM, Haney M, Batrakova E, Kabanov AV. Macrophage exo as natural nanocarriers for protein deliver flamed brain. Biomaterials 2017; 142: 1-1.
- ZHANG W, Yu ZL, Wu M, REN JG, XIA HF, ZHU JY, PANG DW, ZHAO YF, CHEN G. Magnetic

- folate functionalization enables rapid isolation and enhanced tumor-targeting of cell-derived microvesicles. ACS Nano 2017; 11: 277-290.
- 20) SIMONS M, RAPOSO G. Exosomes--vesicular for intercellular communication. Curr ol 2009; 21: 575-581.
- 21) THERY C, OSTROWSKI M, SEGURA E mbrane vesicles as conveyors of immune religions. Nat Rev Immunol 2009; 9: 581-593
- 22) Munagala R, Aoil F, Jeyab J, Agraw Mudd AM, Kyakulaga AH, Sir JP, Vadhanam Ta RC. Exosomal for allation of anthocyal against multiple control types ancer Lett 20.7; 393: 94-102.
- 23) Munagala R, F, Jeya Gupta Bovine milk-derive cosomes for deli y. Cancer Lett 2012 48-61.
- 24) ZHU L MAD GANGADARAN P, H JM, LEE HW, BAEK SM, JEONG F SW, LEE J, AHN BC. Exosomes derived from the val killer cells exert therefore in mela. Theranostics 2017; 7: 2735–2745.
- TIAN Y, LI S, SONG J, JI T, ZHU M, ANDERSON GJ, WEI J, NIE G. A dox bicin delivery platform using engineered nature membrane vesicle exosomes for therapy. Biomaterials 2014; 35:
- 26) We detectroporation: a general phenomenon for manipulating cells and tissues. J Cell Bioma 1993; 51: 426-435.
- AN KE, DWYER RM. Engineering exosomes for cancer therapy. Int J Mol Sci 2017; 18: 1122.